Analytical and innovative solutions for heat transfer problems involving phase change and interfaces

The heat-balance integral: 2. Parabolic profile with a variable exponent: The concept, analysis and numerical experiments

Jordan Hristov

Department of Chemical Engineering, University of Chemical Technology and Metallurgy, 1756 Sofia, 8 Kl. Ohridsky Blvd., Bulgaria

A R T I C L E I N F O	A B S T R A C T
	A heat-balance integral method employing a parabolic profile with a variable (self-adapting) exponent has been developed. The parabolic profile satisfies both the boundary conditions and the heat-balance integral at any value of the exponent, while the optimal solution requires minimization of the mean-squared error defined by the domain parabolic equation. The concept of a variable exponent results in simple relationships involving the *LambertW* function and the initial values defined through the profile calibration at $x = 0$. Two simple 1-D problems with classic solutions are developed to demonstrate the method. © 2012 Académie des sciences. Published by Elsevier Masson SAS. All rights reserved.

1. Introduction

The heat-balance integral of Goodman [1] is one of the leading techniques among the approximate methods in solving 1-D transient diffusion problem over 50 years and is still being developed [2–7]. The thermal penetration depth and prescribed temperature profile transforms strong non-linear 1-D heat conduction problems into ordinary differential equations with respect to the thermal layer front evolution [1,8]. The function approximating the temperature profile across the thermal layer $\delta(t)$ [1,2] should satisfy the following boundary conditions (prescribed temperature and prescribed flux at $x = 0$). The concept of the thermal penetration depth, the problem is defined as

$$\frac{\partial T(x,t)}{\partial t} = \alpha \frac{\partial^2 T(x,t)}{\partial x^2}, \quad 0 \leqslant x \leqslant \delta(t) \tag{1}$$

$$T(0,t) = T_s \quad \text{or} \quad -\lambda \frac{\partial T}{\partial x} = \dot{q}_s \tag{2a}$$

$$T(\delta, t) = T_\infty \tag{2b}$$

$$\lambda \frac{\partial T}{\partial x}\bigg|_{x=\delta} = 0 \tag{2c}$$

$$\frac{\partial^2 T}{\partial x^2}\bigg|_{x=\delta} = 0 \tag{2d}$$

$$\delta(t = 0) = 0 \tag{3}$$

Nomenclature

$A_1(m)$	term of Eq. (11) defined by Eq. (8)
$A_2(m)$	term of $z_2(t)$ defined by Eq. (8) and used in Eq. (11)
a	term in the generalized parabolic profile (Eq. (5))
b	coefficient in the generalized parabolic profile (Eq. (5))
C_1 and C_2	integration constants (see Eqs. (10) and (12))
c	coefficient in the generalized parabolic profile
$D(n, \eta)$	difference between the exact and the approximate solutions
$j(\eta)$	function defined by Eq. (18)
k_j	weighting coefficient in Eq. (18)
$LambertW(z)$	Lambert function
L_1 and L_2	norms defined by Eqs. (19a), (19b)
$m = x/\delta$	collocation point
n	exponent of the parabolic profile
n_0	exponent defined at $x = 0$
n_M^T	exponent defined by the Myers' method
q	heat flux density .... W/m^2
q_s''	surface heat flux ($x = 0$) .... W/m^2
T	temperature .... K
T_a	approximate profile
T_∞	temperature of the undisturbed medium ... K
t	time .... s

x	space co-ordinate .... m
z	argument of $LambertW(z)$ defined by Eq. (10) and Eq. (12)

Greek letters

α	thermal diffusivity .... m^2/s
δ	thermal penetration depth .... m
$\eta = x/\sqrt{\alpha t}$	similarity variable
η	similarity method
λ	thermal conductivity .... W/m K
Θ	dimensionless temperature

Superscripts

s	surface (at $x = 0$)
T	prescribed temperature problem
q	prescribed flux problem

Subscripts

0	defined at the surface ($x = 0$)
a	approximate
e	exact
M	Myers' method
pw	pointwise
W	calculated through the $LambertW$ function

The integration over the domain with respect to the space variable yields:

$$\frac{d}{dt} \int_0^\delta T_a \, dx - T_a(x = \delta) \frac{d\delta}{dt} = -\alpha \frac{\partial T(x, t)}{\partial x} \bigg|_{x=0} \tag{4}$$

The first term of (4) is the heat-balance integral of Goodman [1].

The problem at issue is the use of a $T_a(x, t)$ with unspecified exponent $T_a(x, t) = a + b(1 + cx)^n$ very often used in the form

$$\Theta = \frac{T(x, t) - T_\infty}{T_s - T_\infty} = \left(1 - \frac{x}{\delta}\right)^n \tag{5}$$

This profile satisfies all boundary conditions (1) and the heat-balance integral (4) for every value of the exponent n [9].

The proper choices of the exponent have been analyzed in [9,10] using the principle concept that its value is constant over the entire thermal layer ($0 \leqslant x \leqslant \delta(t)$). The methods determining the profile exponent have been developed on the basis of calibration by the exact solution [9–11], fractional boundary conditions [12], and minimization of the mean-squared error of the domain equation (1) [12,13].

The results provided by Myers [13] with the mean-squared error minimization clearly revealed that the error of approximation depends on the time. This problem, solved with respect to the profile exponent indicates that the profile exponent is time-dependent, that is, it varies as the thermal layer depth $\delta(t)$ grows in time.

The present work focus the attention of the concept that the exponent of the profile (5) depends on time with an initial value defined at any time at $x = 0$.

2. Variable exponent of the parabolic profile

2.1. Basic assumptions – a collocation approach

The hypothesis underlying the analysis is that n depends on the time but is independent on the space variable x. Besides, the approximate profile matches the exact solution and satisfies domain equation (3) at a given point $m = x/\delta$ (*a collocation condition*). With the prescribed temperature problem ($T = T_s$ at $x = 0$), for instance, the profile can be expressed as

$$T_a(x, t) = T_\infty + (T_s - T_\infty)(1 - m)^n, \quad x = m\delta, \ 0 \leqslant m(x) \leqslant 1 \tag{6}$$

Hence, with $n = n(t)$ and taking into account that $\mathrm{d}a^z/\mathrm{d}z = a^z \ln a$ we have from (6):

Denoting $1 - m = p$ and taking into account that $\delta^2 = 2(\alpha t)n(n+1)$ we get

$$\left[(1-m)^n \ln(1-m) \frac{\mathrm{d}n}{\mathrm{d}t} - \alpha n(n-1)(1-m)^{n-2} \frac{1}{\delta^2} \right] = 0 \tag{7}$$

Denoting $1 - m = p$ and taking into account that $\delta^2 = 2(\alpha t)n(n+1)$

$$\frac{\mathrm{d}n}{\mathrm{d}t} = A_1 \frac{(n-1)}{2(n+1)} \frac{1}{t} \tag{8a}$$

$$A_1 = \frac{1}{2}\left(\frac{1}{\ln p} \right) \frac{1}{p^2} \tag{8b}$$

The solution of (9) with respect to n is therefore:

$$n(t) = 1 + 2\,LambertW\left[\frac{1}{2} t^{(\frac{1}{4})A_1} \exp\left(\frac{C_1}{4} A_1 - \frac{1}{2} \right) \right] = 1 + 2\,LambertW(z_1) \tag{9}$$

$$z_1 = z_1(m, t) = \left[\frac{1}{2} t^{(\frac{1}{4})A_1} \exp\left(\frac{C_1}{4} A_1 - \frac{1}{2} \right) \right] \tag{10}$$

where C_1 is an integration constant and $A_1 = A_1(m)$.

Similarly, for the prescribed flux problem ($q_0 = -\lambda \partial T/\partial x|_{x=0}$ at $x = 0$), we have

$$\left[(1-m)^n \ln(1-m) \frac{\mathrm{d}n}{\mathrm{d}t} - \alpha n(n-1)(1-m)^{n-2} \frac{1}{\delta^2} \right] = 0 \tag{11}$$

The solution of (12) with respect to n is

$$n(t) = 1 + 2\,LambertW(z_2) \tag{12}$$

where the $z_2 = z_2(m, t) = [\frac{1}{2} t^{(\frac{1}{4})A_2} \exp(\frac{C_2}{4} A_2 - \frac{1}{2})]$, where $A_2 = A_2(m)$ depends on the choice of m.

2.2. Some comments on the solution concerning the time-dependence of the exponent

Because the point $x/\delta = m$ could be any point of the profile, let us assume for simplicity $x/\delta = m = 1/2$ which denotes the middle point of the thermal layer. Then for $p = 1 - m = 0.5$ and $A_1 = 2/\ln 0.5 \approx -2.885$, $LambertW(z) = ze^z$ for $z_{(m=0.5)} \approx 0.5t^{-0.721}$. Similarly, for $m = 0.3$ we get: $p = 0.7$, $A_1 = -15.575$ and $z_{(m=0.3)} \approx 0.5t^{-3.893}$. For $m = 0.75$ near the front of the thermal layer, $z_{(m=0.75)} \approx 0.5t^{-1.442}$. Therefore, the argument of the Lambert function depends on m and t, i.e. $z = z(x, t)$. However, this complicates the form of the functional relationship since in this case, $n = n(x, t)$. This can be successfully used if the solution should attain a minimum error at a given point of the thermal layer, at $x/\delta = m = 0.5$, for instance.

2.3. Direct approach to the relationship $n(\eta)$ and numerical tests

Thanking into account that HBI solution can be expressed through the similarity variable $\eta = x/2\sqrt{\alpha t}$ in the form $\Theta_a = (1 - \eta/F)^n$ ($F_T = \sqrt{2n(n+1)}$ for the prescribed temperature at $x = 0$, while $F_q = \sqrt{n(n+1)}$ for prescribed flux at $x = 0$). We introduce the pointwise error of the approximation as $D_{pw}(n, \eta) = \Theta_e - \Theta_a$, where the exact solutions are [14]:

- *For prescribed temperature problem*

$$\Theta_e^T = 1 - \mathrm{erf}(\eta/2) \tag{13}$$

- *For the prescribed flux problem*

$$\Theta_e^q = 2\left[\mathrm{ierfc}\left(\frac{\eta}{2} \right) \right] \tag{14}$$

Then, setting $D_{pw}(n, \eta) = 0$ we get a non-linear equation that can be solved with respect to n, at a given value of the similarity variable η. Setting different values of η in the range $0.1 \leqslant \eta \leqslant 6$ we got values of n (by Maple 13) exhibiting different behaviors depending on the range of η. Two approximations were done, for the prescribed temperature problem, for example:

$$n^T = 0.266 + 0.649\eta, \quad 1 \leqslant \eta \leqslant 6 \tag{15}$$

$$n^T = 1.888 + 0.036 \exp(6.796\eta), \quad 0.1 \leqslant \eta \leqslant 0.9 \tag{16}$$
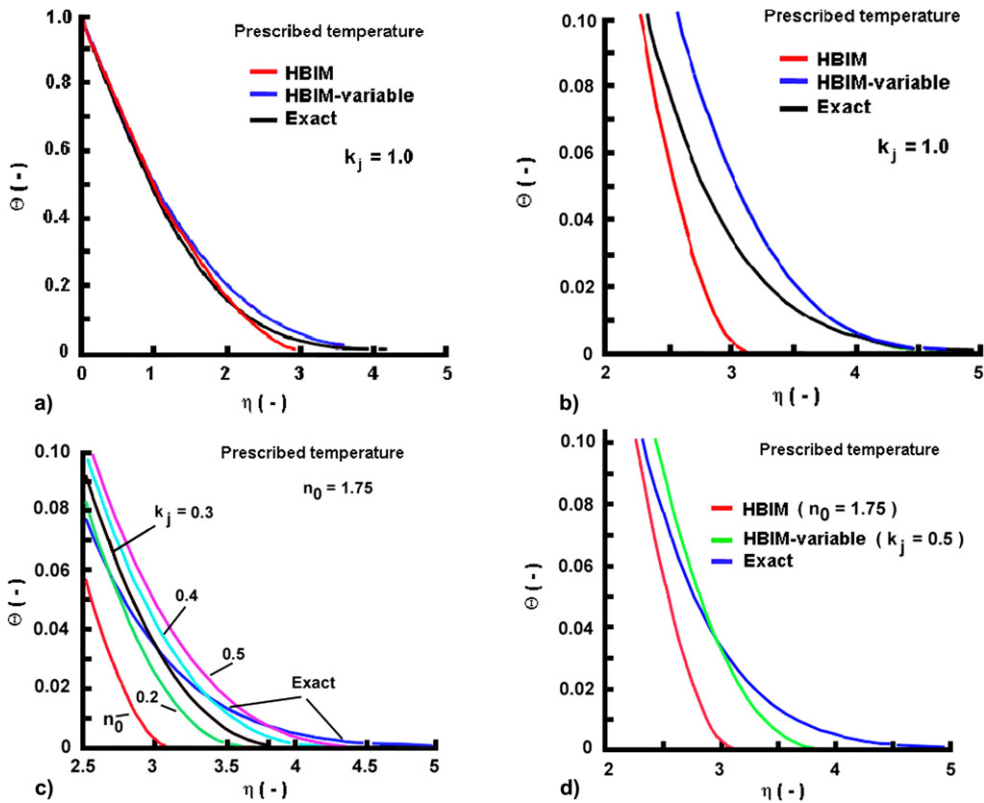
Fig. 1. Numerical experiments with the approximate profile obtained for the prescribed temperature problem. Fixed exponent (**HBIM**); Variable exponent (**HBIM-variable**); Exact solution (**Exact**). (a) Profiles over the entire range of variations $0 \leqslant \eta \leqslant 6$ with $k_j = 1.0$ in the approximate solution. (b) Profiles in the range $2 \leqslant \eta \leqslant 5$ with $k_j = 1.0$ in the approximate solution. (c) Profiles in the range $2 \leqslant \eta \leqslant 5$ demonstrating the effect of the weighting coefficient k_j. (d) Profiles in the range $2 \leqslant \eta \leqslant 5$, $k_j = 0.5$.

The upper range $\eta = 6$ was chosen from practical reasons because $\Theta_e^T(\eta = 6) \approx 0.0002$, that is almost the front of the thermal layer. The point $\eta = 0$ was excluded because at $x = 0$, the exponent can be calibrated directly through the exact solution, as it was demonstrated elsewhere [9–11]. From Eq. (16), setting $\eta \to 0$ we may extrapolate $n \to 1.924$, that is between the value obtained through calibration at $x = 0$, i.e. $n_0^T = 1.75$ [9,11] and the that obtained through the mean-squared error approach: $n_M^T \approx 2.235$ (the Myers's approach [13]) and $n_\eta^T \approx 1.507$ [12].

Similarly, for the prescribed flux problem, by using the exact solution (14), and setting $D_{pw}(n, \eta) = 0$, we got two sets of values of n. The solutions in this case with $\eta \geqslant 1.5$ are straightforward and provide reasonable values of the exponent n. Unfortunately, for $\eta \leqslant 1.5$, more precisely for $0 \leqslant \eta \leqslant 1$, Maple numerical solution provides extremely high values of n which are practically unacceptable. Because of that, only those values of n obtained for $\eta \geqslant 1.5$ where approximated to establish the trend in the relationship $n = n(\eta)$. They were approximated by

$$n^q = 3.602 + 0.478 \exp(0.423\eta), \quad 1.5 \leqslant \eta \leqslant 6 \tag{17}$$

As $\eta \to 0$ we extrapolate $n \approx 3.602$ that is close to $n_0^q = 3.65$ established by direct calibration to the exact solution [14] and by the fractional boundary condition applied to the profile [12], but lower than $n_M^q \approx 3.854$ obtained by Myers [13].

Relationship (17) as well as (15) and (16) should be considered as outcomes of direct experiments matching the approximate HBIM profiles and the exact solutions and their use is possible, to some extent, in practical cases. However, the principle question is: what is the upper limit of the time t in the parabolic profile, because the exponent should be in the range established. This question comes naturally from (15), (16) and (17) where the exponent is not limited from above (i.e. $n(t) \to \infty$) as the time goes on. This ambiguity is avoided by the self-adaptive exponent depending on the similarity variable, as it is presented next.

2.4. Self-adaptive exponent $n(\eta)$ and numerical tests

The outcomes of the collocation approach and the direct numerical test indicate that the correction to initial value n_0 should grow almost exponentially as the depth of the thermal layer increases. Hence, a general expression of the variable exponent can be suggested as
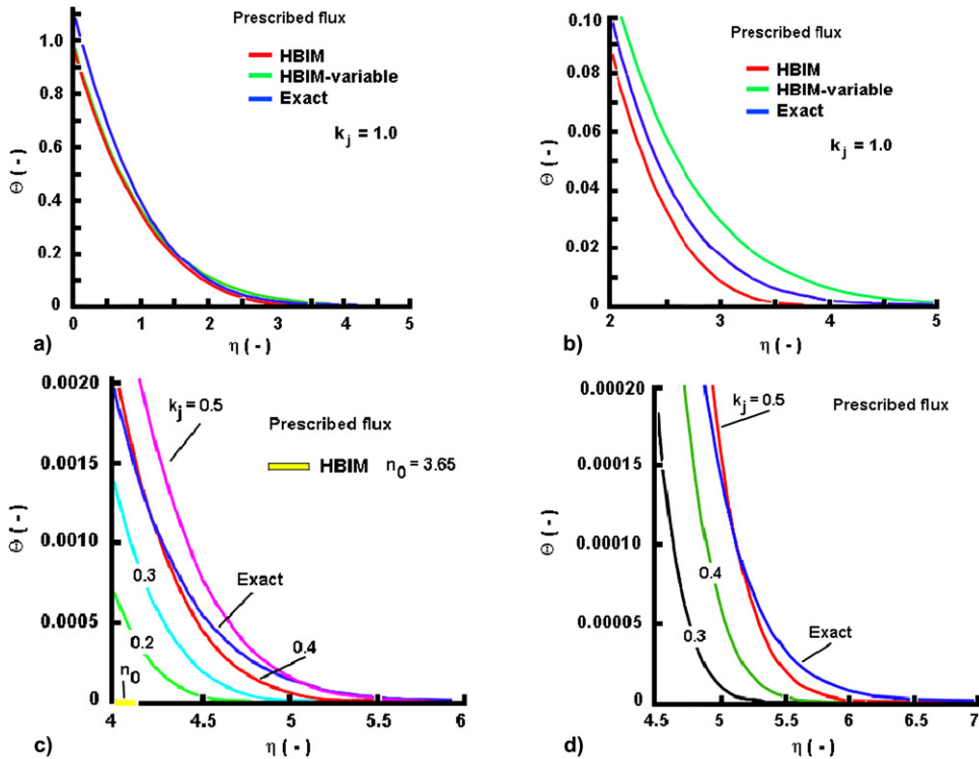
Fig. 2. Numerical experiments with the approximate profile obtained for the prescribed flux problem. Fixed exponent (**HBIM**); Variable exponent (**HBIM-variable**); Exact solution (**Exact**). (a) Profiles over the entire range of variations $0 \leqslant \eta \leqslant 6$ with $k_j = 1.0$ in the approximate solution. (b) Profiles in the range $2 \leqslant \eta \leqslant 5$ with $k_j = 1.0$ in the approximate solution. (c) Profiles close to the edge of the thermal front (defined by the exact solution) demonstrating the effect of the weighting coefficient k_j. (d) Profiles in the range $4.5 \leqslant \eta \leqslant 7 k_j$.

$$n = n_0 j(\eta), \quad j(\eta) = 1 + k_j \, LambertW(\eta) \tag{18}$$

concerning the positive branch of the Lambert function.

Because for the Lambert function $W(\eta)e^{W(\eta)} = \eta$ we have $W(0) = 0$, the correction $j(\eta)$ provides $n(0) = n_0$ thus matching the exact solution at $x = 0$.

Plots of the HBIM profiles with the self-adaptive exponents are shown in Figs. 1 and 2. The approximate profiles with adaptive exponents go closer (slightly underestimating) to the exact solutions within the range $0 \leqslant \eta \leqslant 2$ (see Figs. 1a, 1b and Figs. 2a, 2b) with $k_j = 1$. However, beyond $\eta \approx 2$, and going to the edge of the thermal layer, the effect of the right choice of k_j becomes more significant (see Figs. 1b and 2b). In general, the approximate profiles come close to the exact solutions as k_j approaches $k_j \approx 0.5$ from the left ($0 < k_j \leqslant 0.5$) and go away as $k_j > 0.5$, as it is shown in Figs. 1c and 2c. The numerical tests performed allow suggesting that $k_j = 0.5$ can be used in both approximated profiles discussed here over the entire range of variations of η. To some extent, at the edge of the thermal layer (i.e. $\eta > 4$) $k_j \approx 0.4$ leads to a better approximation of the prescribed flux problem profile (see Figs. 2c and 2d), while $0.4 < k_j < 0.6$ works better for the prescribed temperature problem (Figs. 1c and 1d). However, the differences with respect to the case with $k_j = 0.5$ are negligible taking into account the global error of approximation of the heat-balance integral method.

In addition, we notice that the average values of the exponents calculated through (18), over the range $0 \leqslant \eta \leqslant 6$, for the prescribed temperature problem, have a mean of $\langle n_W^T \rangle \approx 2.121$ which is quite close to that established by Myers' $n_M^T \approx 2.235$ [13]. Similarly, for the prescribed flux problem, we have a mean of $\langle n_W^q \rangle \approx 4.0036$. These are only statistical estimates, so we have to estimate next the errors of approximations established through the L_1 and L_2 norms.

2.5. Error of approximation

The pointwise error of approximation (14) allows defining the L_1- and L_2-norm of errors as

$$e_{L_1} = \int_0^\delta |\Theta_a - \Theta_e| \, dx, \qquad e_{L_2} = \int_0^\delta (\Theta_a - \Theta_e)^2 \, dx \tag{19a}$$

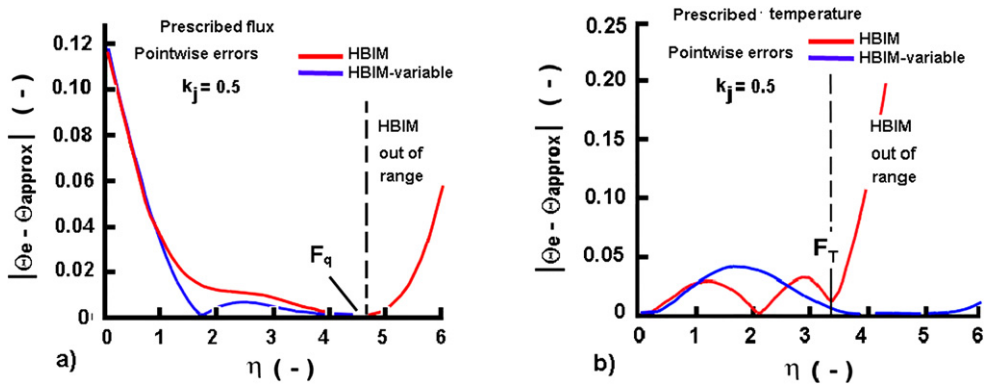Using the similarity variable $\eta = x/\sqrt{\alpha t}$, the above can be expressed as

Fig. 3. Pointwise errors of approximation for both classical HBIM and modified HBIM with a variable exponent $k_j = 0.5$. (a) Prescribed flux problem. (b) Prescribed temperature problem.

Table 1
Errors in approximation with the HBIM profiles-prescribed temperature problem.

Norm	Fixed exponent[a]	Variable exponent[b]					
		$k_j = 0.2$	$k_j = 0.4$	$k_j = 0.5$	$k_j = 1$	$k_j = 1.2$	$k_j = 1.5$
$L_1 \times 10^3$	56.33	51.85	68.14	76.25	101.94	108.167	11.51
$L_2 \times 10^3$	1.33	1.257	1.979	2.49	4.47	5.134	5.9

[a] The upper limit of integration is $y = F_n = \sqrt{2n_0^T(n_0^T + 1)} = 3.102$.

[b] The upper limit of integration is $\eta = 6$.

Table 2
Errors in approximation with the HBIM profiles-prescribed flux problem.

Norm	Fixed exponent[a]	Variable exponent[b]					
		$k_j = 0.2$	$k_j = 0.4$	$k_j = 0.5$	$k_j = 1$	$k_j = 1.2$	$k_j = 1.5$
$L_1 \times 10^3$	113.465	94.2	94.972	98.4	114.78	119.933	126.388
$L_2 \times 10^3$	7.309	1401.9	7.106	7.146	7.479	7.626	1401.914

[a] The upper limit of integration is $y = F_n = \sqrt{n_0^q(n_0^q + 1)} = 4.119$.

[b] The upper limit of integration is $\eta = 6$.

$$e_{L_1} = \int_0^{F_n} |\Theta_a - \Theta_e|\, d\eta, \qquad e_{L_2} = \int_0^{F_n} (\Theta_a - \Theta_e)^2\, d\eta \qquad (19b)$$

The pointwise errors as functions of the similarity variable are shown in Fig. 3. For the prescribed flux problems (see Fig. 3a) the HBIM profiles with either fixed or variable exponents exhibit similar pointwise errors in the range $0 \leqslant \eta \leqslant 1$. Beyond this range the error of the profile with the variable exponent is significantly lower than that exhibited by fixed exponent approximation. For the prescribed temperature problem (Fig. 3b) the error of the profile with a variable exponent is comparable or slightly greater than that with the fixed exponent with $0 < \eta < 3.5$. Beyond $\eta \approx 3.5$ the profile with variable exponent is better. The upper limits of integration in (19b) are different for the fixed and the variable exponent solutions. More precisely, the upper limits for the profiles with fixed exponents are $F_T(n_0) = \sqrt{2n_0^T(n_0^T + 1)}$ and $F_q(n_0) = \sqrt{n_0^q(n_0^q + 1)}$. Beyond these points these HBIM profiles are no longer valid. With the variable exponent, the upper limit of integration was chosen as $\eta = 0.6$ because $\lim_{\eta \to 6} \Theta_a \approx 1.0194 \times 10^{-5}$, that practically matches the exact solutions and the real front of the penetration layer, irrespective of the problem at issue.

The final choice, however, should be made based on the L_1- and L_2-norm errors (see Tables 1 and 2). The effect of the weighting coefficient k_j on both L_1 and L_2 norms is obvious: the better approximations correspond to $0.4 < k_j < 0.5$. This work does not investigate the value of k_j because from a practical point of view either $k_j = 0.4$ or $k_j = 0.5$ can be used without significant effect on the approximate solution. From author's experience with the numerical experiments performed, $k_j = 0.5$ leads to better results even though both the L_1 and L_2 norms with $k_j = 0.4$ are lower. The latter suggestion is based on the fact, that beyond the point where the HBIM with fixed exponent ends, the self-adaptive profiles with $k_j = 0.5$ demonstrate lower pointwise errors that those with $k_j = 0.4$. The L_1 and L_2 norms are global measures of the approximation over the entire domain, while the pointwise error directly shows how close the approximate solution is

to the exact one over a certain range of variation of the variable. In cases when exact solutions are not available, then the L_1 and L_2 norms are the only on hand to take the decision. From a practical point of view, the expressions of the L_2 norm (the classic approach) are cumbersome and those of the L_1 norm can be used, taking into account that under the absolute value of the pointwise error is the integral sign. This leads to simpler expressions and practical results about the error of approximation as the similarity variable increases.

3. Discussion

The present work conceives the idea of a heat-balance integral method employing a parabolic profile with self-adaptive exponent. The numerical experiments with HBIM profiles expressed through $\eta = x/\sqrt{\alpha t}$ clearly show that the approximate solution does not follow the exact one as the time goes on and the exponent should vary as η increases. The present work has demonstrated this by two numerical experiments: (1) The collocation condition requiring the approximate profile to match the exact solution at one point of the thermal layer; (2) Direct solution of the pointwise error with respect to the exponent n. Both attempts reveal that the exponent depends on the space variable and the time explicitly (the collocation approach) or implicitly through the similarity variable. The second approach shows more clearly, what the behavior of the exponent should be as the similarity variable increases.

As a general rule, accepted from the outcomes of both attempts, a relationship of a self-adaptive exponent was conceived. The self-adaptive correction is based on the *LambertW* function with the similarity variable as argument. All experiments and the analyses of the both the L_1- and L_2-norm errors reveal that the parabolic profile with a self-adaptive exponent approximates better the temperature profiles than the classical HBI method with fixed exponent. Moreover, the self-adaptive profile works beyond the limit established by the classical HBIM towards the thermal layer front determined by the exact solution.

The suggested profile, in fact, draws a new approach in the design of the HBIM profiles and shows a straightforward algorithm how the self-adaptive exponent can be determined, namely:

(1) Fit the profile provided by temperature (or flux) problem to that provided by the exact solutions (if any) at $x = 0$ and determine the exponent. If exact solution for the particular boundary condition is not available, then fit the profile provided temperature (or flux) to those calculated through fractional half-time derivatives (Riemann–Liouville sense) as it is demonstrated in [12], then determine the exponent at $x = 0$.
(2) Use the exponent defined at $x = 0$ as the initial value of the relationship $n(\eta) = n_0 + k_j LambertW(\eta)$ and create the HBIM profile. The weighting coefficient k_j can be adjusted through minimization of the L_1 and L_2 norms.

4. Conclusions

The concept of self-adaptive parabolic profile of the heat-balance integral method has been conceived. The main outcome can be outlined as:

(1) The exponents established at the boundary $x = 0$ are the initial values of self-adaptive functional relationships based on the *LambertW* function. The numerical simulations performed reveal that the weighting coefficient on *LambertW*-based correction is about 0.4 or 0.5 for both prescribed flux and prescribed temperature problems.
(2) The self-adaptive approximate profiles work beyond the limits established by the classical HBIM towards the thermal layer fronts determined by the exact solutions. It may serve as good tool for developing approximate analytical solutions problems where the temperature profile close to the phase-change interface is of primary importance [15,16].
(3) The L_1 and L_2 norms of the self-adaptive profiles are close to those of the classical HBIM approximate solutions but over wider ranges of variation of the similarity variable.

Acknowledgements

References

[1] T.R. Goodman, The heat balance integral and its application to problems involving a change of phase, Transactions of ASME 80 (1–2) (1958) 335–342.
[2] A.S. Wood, F. Mosally, A. Al-Fhaid, On high-order polynomial heat-balance integral implementations, Thermal Science 13 (2) (2009) 11–25.
[3] V. Novozhilov, Application of heat-balance integral method to conjugate thermal explosion, Thermal Science 13 (2) (2009) 73–80.
[4] N. Sadoun, El-Khider Si-Ahmed, P. Collinet, J. Legrand, On the Goodman heat-balance integral method for Stefan like-problems, Thermal Science 13 (2) (2009) 91–96.
[5] S.K. Sahu, P.K. Das, S. Bhattacharyya, How good is Goodman's heat-balance integral method for analyzing the rewetting of hot surfaces? Thermal Science 13 (2) (2009) 97–112.
[6] A.P. Roday, M.J. Kazmierczak, Analysis of phase-change in finite slabs subjected to convective boundary conditions: Part I – Melting, Int. Rev. Chem. Eng. 1 (1) (2009) 87–99.
[7] A.P. Roday, M.J. Kazmierczak, Analysis of phase-change in finite slabs subjected to convective boundary conditions: Part II – Freezing, Int. Rev. Chem. Eng. 1 (1) (2009) 100–108.

 [8] T.R. Goodman, Application of integral methods to transient nonlinear heat transfer, in: T.F. Irvine, J.P. Hartnett (Eds.), Advances in Heat Transfer, vol. 1, Academic Press, San Diego, CA, 1964, pp. 51–122.

 [9] J. Hristov, The heat-balance integral method by a parabolic profile with unspecified exponent: Analysis and benchmark exercises, Thermal Science 13 (2) (2009) 22–48.

[10] W. Braga, M. Mantelli, A new approach for the heat balance integral method applied to heat conduction problems, in: 38th AIAA Thermophysics Conference, Toronto, Ontario, June 6–9, 2005, paper AIAA-2005-4686.

[11] J. Hristov, Research note on a parabolic heat-balance integral method with unspecified exponent: An entropy generation approach in optimal profile determination, Thermal Science 13 (2) (2009) 49–59.

[12] J. Hristov, The heat-balance integral: How to calibrate the parabolic profile? Comptes Rendus Mecanique 340 (7) (2012) 485–492.

[13] T. Myers, Optimizing the exponent in the heat balance and refined integral methods, Int. Comm. Heat Mass Transfer 36 (2009) 143–147, doi:10.1016/j.icheatmasstransfer.2008.10.013.

[14] H.S. Carslaw, J.C. Jaeger, Conduction of Heat in Solids, 2nd ed., Oxford University Press, Oxford, UK, 1992.

[15] M. El Ganaoui, R. Bennacer, On some latent heat effects on the floating zone growth, Adv. Space Res. 36 (1) (2005) 96–98.

[16] M. El Ganaoui, A. Lamazouade, P. Bontoux, D. Morvan, Computational solution for fluid flow under solid/liquid phase change conditions, Computers & Fluids 31 (4–7) (2002) 539–556.